Supplementary information

Dual spindle formation in zygotes keeps parental genomes apart in early mammalian embryos

Judith Reichmann[1], Bianca Nijmeijer[1], M. Julius Hossain[1], Manuel Eguren[1], Isabell Schneider[1], Antonio Z. Politi[1], Maria J. Roberti[1], Lars Hufnagel[1], Takashi Hiiragi[2] and Jan Ellenberg[1]*

Affiliations:
[1]Cell Biology and Biophysics Unit, European Molecular Biology Laboratory, Meyerhofstrasse 1, 69117 Heidelberg, Germany.

[2]Developmental Biology Unit, European Molecular Biology Laboratory, Meyerhofstrasse 1, 69117 Heidelberg, Germany.

*Corresponding author. E-mail: jan.ellenberg@embl.de

Supplementary Tables

Supplementary Table 1.

Embryo Treatment	Number of Embryos transferred	Total number of live pups born	Number of live pups born in %
None	170	75	44
NocMo	107	45	42
MoNoc	135	66	49

Supplementary Materials and Methods

Mouse strains and embryo culture

For EdU labelling of paternal chromatin male from C57BL/6J x C3H/He mice were supplied continuously with drinking water containing 0.5 mg/ml EdU. The EdU-containing water was changed twice per week. EdU is incorporated in place of thymidine into the replicating DNA of mitotically dividing somatic and pre-meiotic cells. The cycle time to produce mature spermatozoa from EdU-labelled pre-meiotic cells in mice is ~35 days. After continuous EdU feeding for at least 6 weeks,

EdU-treated males were mated with superovulated B6C3F1 females. Embryos were isolated 20 hours after HCG injection and cultured in G1 medium (Vitrolife) up to the 8-cell stage.
Embryos used for live imaging of microtubule tips were isolated from C57BL/6J x C3H/He F1 females mated with C57BL/6J x C3H/He F1 males.

Immunofluorescence

To visualise EdU-substituted DNA embryos were fixed with 1%PFA for 30 minutes and then washed three times in PBS. For staining of EdU labelled DNA embryos were treated with Click-iT® Labelling Technologies (Thermo Fisher Scientific C10340) according to the manufacturer's instructions. Paternal chromatin was labelled with Alexa Fluor 647 and the whole nucleus counter stained with 100nM Sytox Green (Molecular probes S7020).
For immunofluorescence of H3K9me3 and Ring1B embryos were fixed as described [1]. Embryos were incubated overnight at 4 °C at the following primary antibody dilutions: 1:2000 rabbit anti Ring1B (Abcam 101273) or 1:200 rabbit anti-H3K9me3 (Abcam 8898) in 5% normal goat serum, 3% BSA in PBST. Embryos were washed with 0.3%BSA in PBST for 3x 5 minutes then incubated with 1:1000 anti-rabbitAlexa 647 and 5ug/ml Hoechst (Sigma) for 1 hour at room temperature. Embryos were washed with 0.3%BSA in PBST for 3x 5 minutes before imaging.

Embryo Imaging

Fixed EdU treated embryos were imaged using the in-house-built inverted light-sheet microscope. 101 images with 520nm between planes were acquired consecutively for Sytox Green and Alexa 647 signals. Fixed embryos stained for epigenetic marks were imaged on a SP8 Leica confocal microscope equipped with a 63× C-Apochromat 1.2 NA water immersion objective lens. Images were acquired at 90 nm XY and 360 nm Z resolution. For imaging of growing microtubule tips 5 images with 500 nm between planes were acquired simultaneously for mCherry and EGFP at 800 ms intervals using the in-house-built inverted light-sheet microscope.

Image processing and analysis

Segmentation and analysis of EDU signal

The nucleus was segmented from the DNA signal and used as a mask to segment the EdU signal. The centre of nuclear mass was detected and a plane was fitted through the centroid to achieve maximum separation of the EdU signal in the two resulting hemispheres. Then, the volume of the smallest EdU signal was divided by the volume of the largest EdU signal.

Segmentation and analysis of maternal and paternal genomes

The chromosome mass was segmented from the DNA channel and used as mask to crop maternal wand paternal chromosome signals. These signals were then segmented using intensity threshold without considering the regions masked out. Segmented maternal and paternal chromosomes were bounded by two separate 3D convex hulls. The mixing between the two was computed by the volume of overlapping voxels between two convex hulls divided by the volume of the union of the two convex hulls.

Simulation of random distribution of paternal chromatin signal at interphase

Three spheres were generated representing chromosome masses of 2-cell, 4-cell and 8-cell embryos. The average volume of cells in each stage was calculated from the original data in order to select the radius of each sphere to achieve comparable relative volumes of chromosome masses in different stages. 40, 20 and 10 small spheres representing paternal chromatin signal were generated with the chromosome masses of 2-cell, 4-cell and 8-cell embryos, respectively.

Simulation of random distribution of maternal and paternal centromere signals at metaphase

A model for chromosome mass was generated by combining the shape information of several individual metaphase chromosome masses. 40 spheres with the same radius were generated in random location within the model chromosome mass of which 50% represent maternal and 50% paternal chromosomes. A minimum distance between the centroids of any two spheres was enforced in order to avoid generating multiple spheres in the same location.

Correlation of maternal and paternal chromosome congression (15-frame window)

To segment chromosomes, original images were filtered first using a 2D Gaussian filter of size 3 and SD=2. Filtered images were interpolated along Z to obtain isotropic pixel size. Pixels at a distance from the centre of mass >13 μm were discarded to reduce the effect of noisy blobs to be detected as chromosomes. Each slice of the interpolated stack was binarised using an adaptive threshold value determined by combining both 2D and 3D threshold values as described in [2]. Chromosome masses were detected after removing very small and scattered pixels by connected component analysis. Maternal and paternal chromosome masses were represented by their three orthogonal Eigen vectors and associated eigenvalues where the eigenvector with the smallest eigenvalue represented the shortest elongated axis of the chromosomal volume. This smallest Eigen value was used as a measure for chromosome congression over time. Since duration of individual phases in different embryos may vary, they were normalised to average phase time. This resulted in uniform phase wise progression among all the embryos and allowed comparison in time. Correlation (Pearson) of the smallest Eigen values between maternal and paternal chromosomes was computed over time considering a sliding window of size 15.

Correlation between 5mC and 5hmC signals

The Yoyo channel was interpolated first to obtain isotropic voxels. A 3D Gaussian filter of size 3 and SD=2 was applied to reduce the effect of noise. Interpolated stacks were binarised by combining 2D and 3D threshold values and chromosome masses were detected by connected component analysis. Interpolated slices were removed to keep only original slices in order to detect 5mC and 5hmC signals inside the chromosome mass. Spatial correlation between these two signals was performed considering only their bright pixels (top 25%) detected from their histograms. Then their correlation were computed as below

$$\frac{N_{5mC \cap 5hmC}}{\sqrt{N_{5mC} \times N_{5hmC}}}$$

Where N_{5mC} and N_{5hmC} represent the number of 5mc and 5hmC top 25% positive pixels, respectively.

Volume occupied by Top 50% of pixels for 5mC, 5hmC, Ring 1B and H3K9me3

Segmentation of 5mC, 5hmC, Ring1B and H3K9me3 regions was performed as described above, however a number of top pixels that added up 50% of the total intensity of the signal were selected. The volume occupied by these pixels was divided by the total volume of the signal.

Average intensity for maternal and paternal pro-nuclei 5mC and 5hmC labelling

Chromosome regions were segmented from the DNA channel. The average background intensity was calculated from the intensity in chromosome free regions and was subtracted from the original signal. The average intensity of pro-nuclei was calculated from the background subtracted signal.

Analysis of directionality of growing microtubule tips

To analyse the directionality of growing microtubule tips the Laplacian of Gaussian, also known as the Mexican hat filter, was computed using the ImageJ plugin LoG3D [3]. Kymographs were computed using the kymograph analyze feature of ImageJ (Rasband, W.S., ImageJ, U. S. National Institutes of Health, Bethesda, Maryland, USA, https://imagej.nih.gov/ij/, 1997-2016.).

EB3 comets were tracked using the Matlab tool u-track2.0 from the Danuser Lab (www.utsouthwestern.edu/labs/danuser/software/). Due to the 4D nature of the problem the track length was typically short with approximately 80% of the tracks shorter than 5 frames. For the analysis we used tracks longer than 3 frames that were sufficient to determine the overall direction of microtubule growth, resulting in > 7000 tracks per embryo. As the tracks followed straight lines, we used the vector determined by the initial and end point of the track for further processing. To remove tracks from astral microtubules we performed a density based clustering using the average track position and chose the largest cluster (Michael Hahsler and Matthew Piekenbrock (2017). dbscan: Density Based Clustering of Applications with Noise (DBSCAN) and Related Algorithms. R package

version 1.1-1. https://CRAN.R-project.org/package=dbscan). To cluster similar trajectories (Supplementary Fig. 3B) we performed spectral clustering using the absolute cosine distance between trajectories to construct the similarity matrix (David Meyer and Christian Buchta (2017). proxy: Distance and Similarity Measures. R package version 0.4-17. https://CRAN.R-project.org/package=proxy). Then we computed eigenvalues and eigenvectors of the random-walk normalised graph-Laplacians (Chung, F. (1997). Spectral graph theory (Vol. 92 of the CBMS Regional Conference Series in Mathematics). Conference Board of the Mathematical Sciences, Washington.). The Eigen gapheuristic indicated that three clusters were sufficient to describe our data (not shown).

1 Kitajima, T. S., Ohsugi, M. & Ellenberg, J. Complete kinetochore tracking reveals error-prone homologous chromosome biorientation in mammalian oocytes. *Cell* **146**, 568-581, doi:10.1016/j.cell.2011.07.031 (2011).

2 Heriche, J. K. *et al.* Integration of biological data by kernels on graph nodes allows prediction of new genes involved in mitotic chromosome condensation. *Mol Biol Cell* **25**, 2522-2536, doi:10.1091/mbc.E13-04-0221 (2014).

3 Sage, D., Neumann, F. R., Hediger, F., Gasser, S. M. & Unser, M. Automatic tracking of individual fluorescence particles: application to the study of chromosome dynamics. *IEEE Trans Image Process* **14**, 1372-1383 (2005).

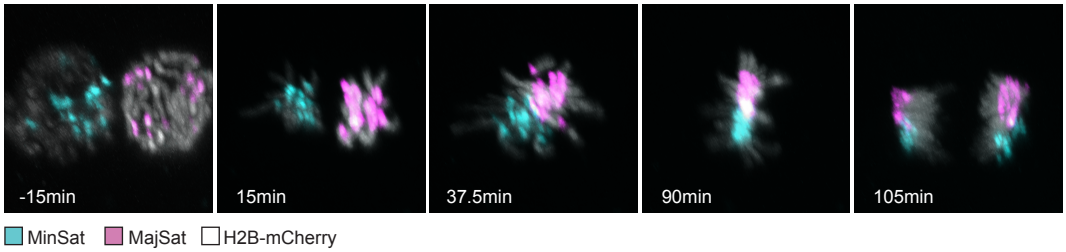

Supplementary Figure 1

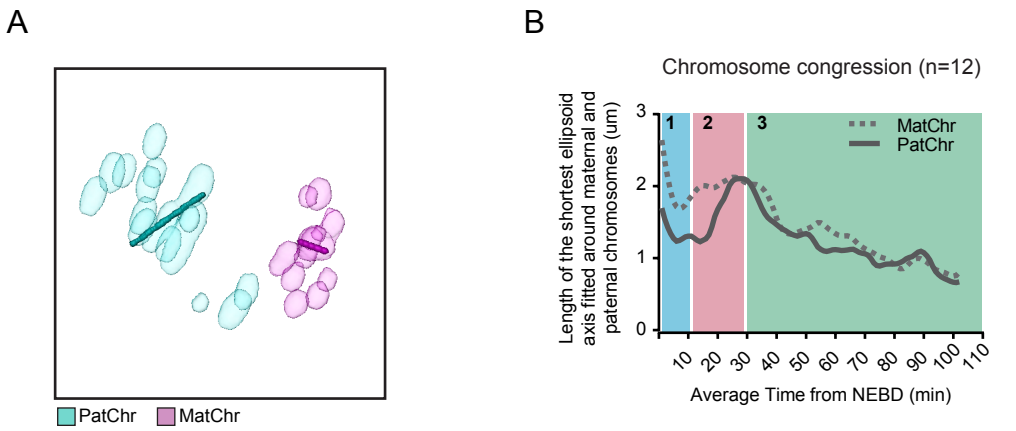

Supplementary Figure 2

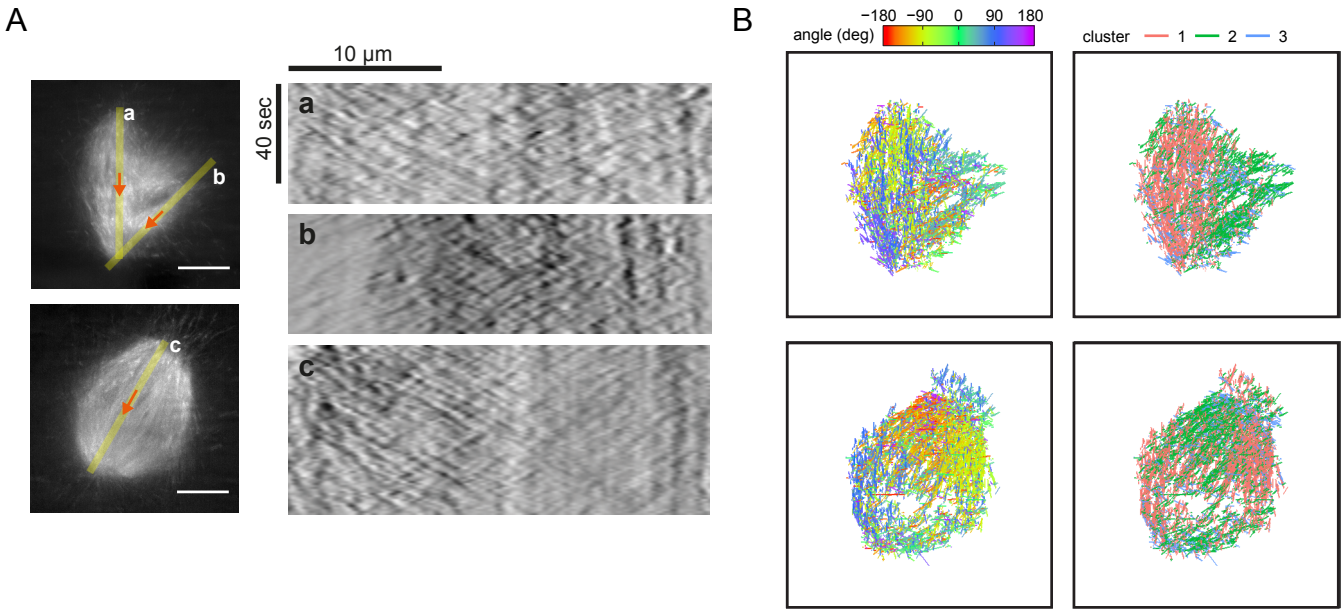

Supplementary Figure 3

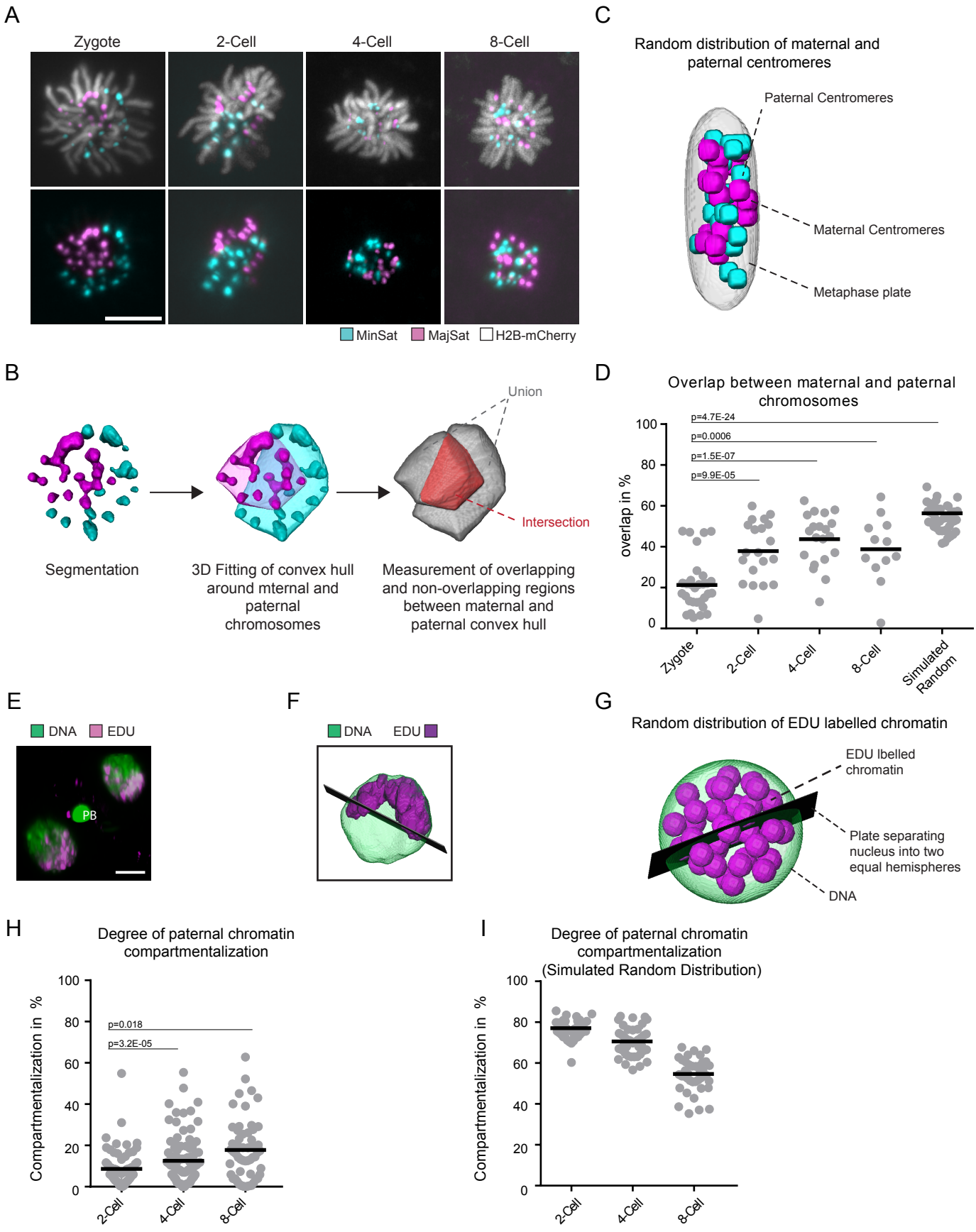

Supplementary Figure 4

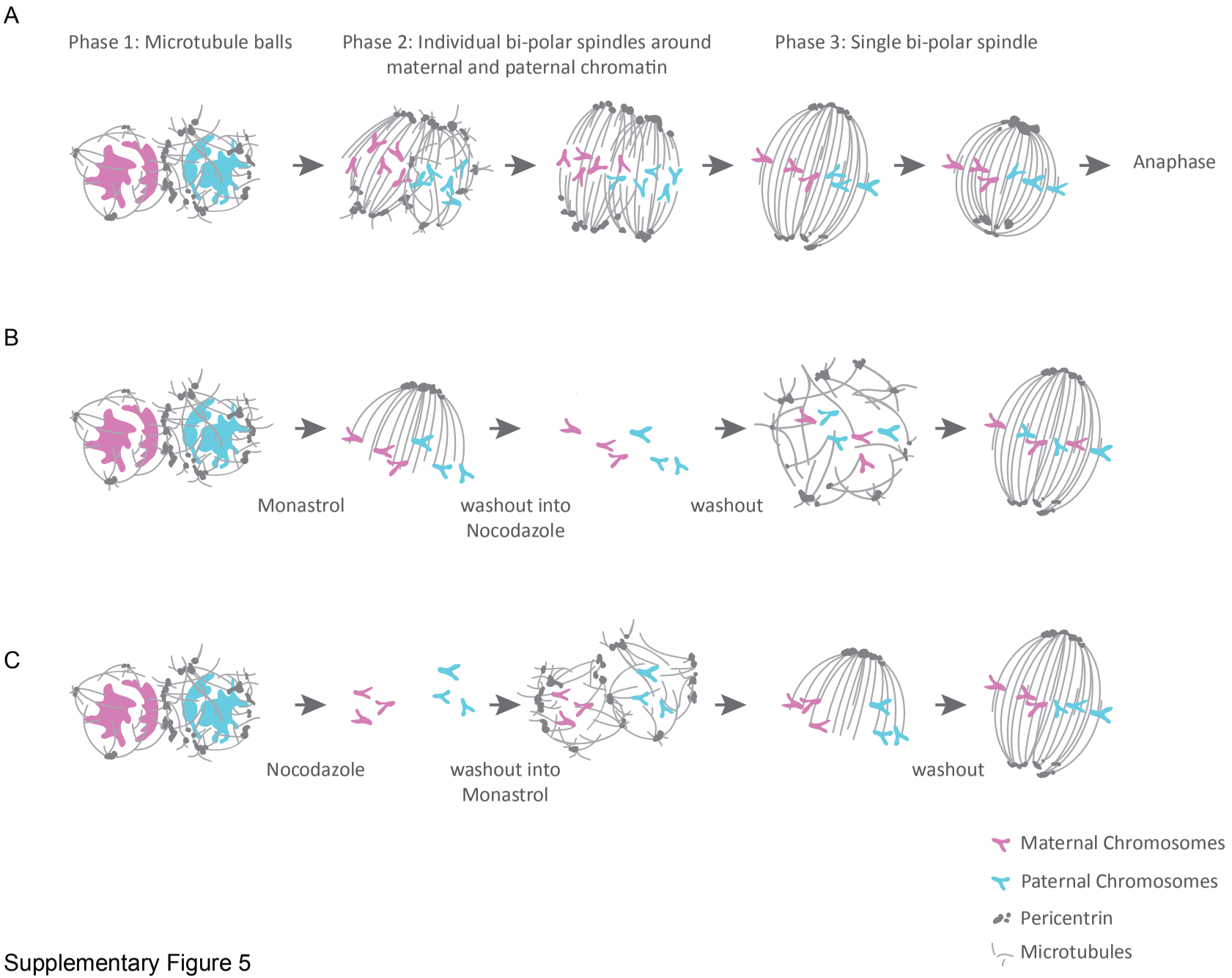

Supplementary Figure 5

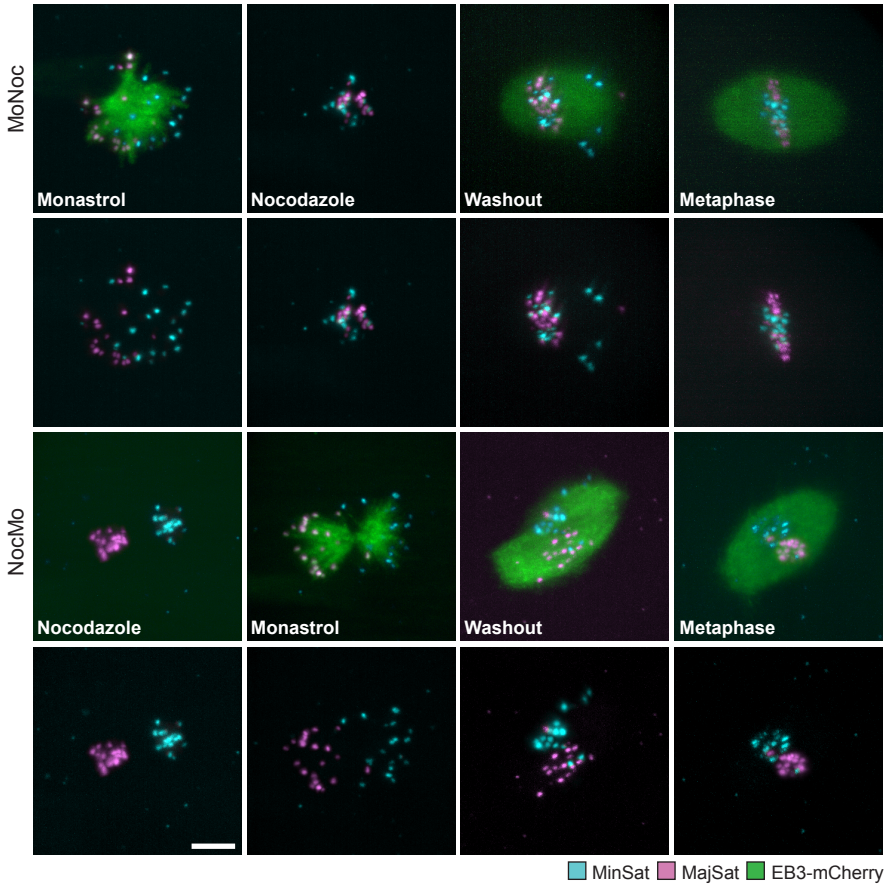

Supplementary Figure 6

A

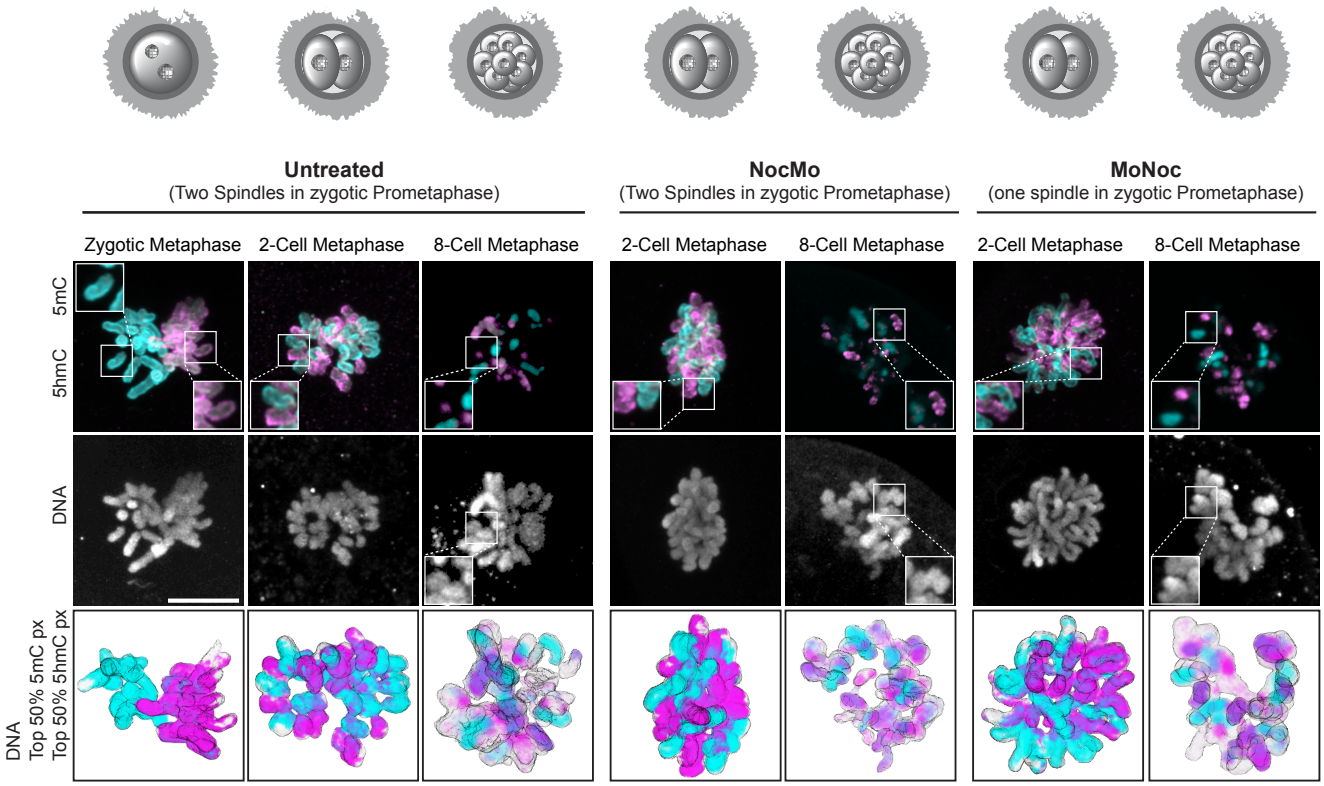

B

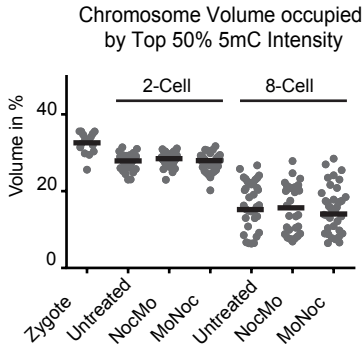

C

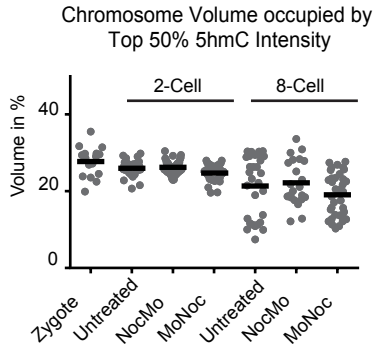

Supplementary Figure 7

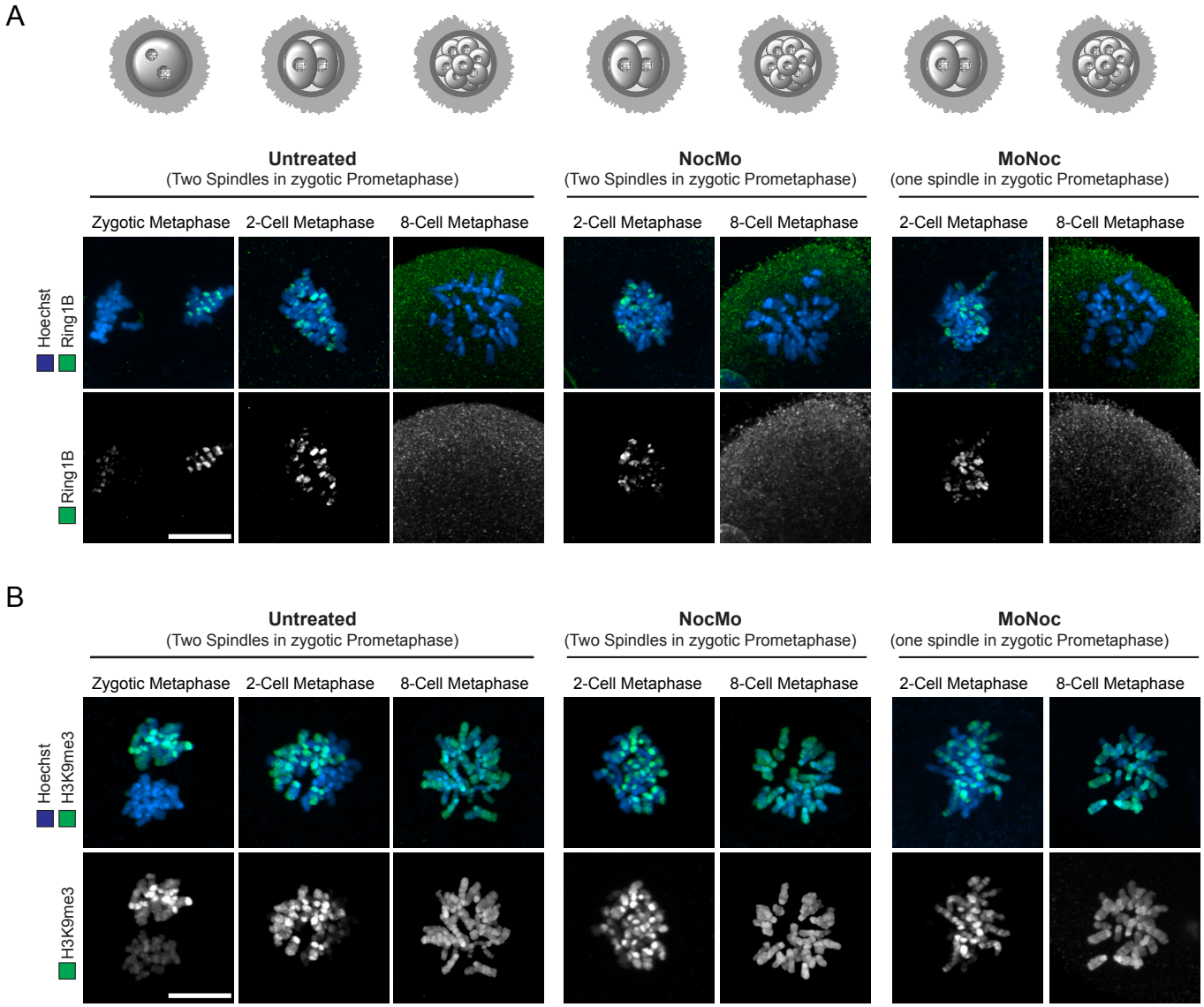

Supplementary Figure 8

Supplementary Figures

Supplementary Figure 1. Distribution of parental chromosomes in mouse zygotes. Differential labelling of maternal (magenta) and paternal (cyan) centromeres through distinction of minor and major satellite regions by fluorescent TALEs. Chromosome arms are labelled with H2B-mCherry (grey). Representative z-projected images of parental chromosome distribution at different time points during the first mitosis of live imaged MMU x MSPS zygotes are shown. NEBD is time point 0.

Supplementary Figure 2. Bi-polar spindle formation around each pronucleus (MMU x MSPS zygotes). (A) Schematic of ellipsoid fitting to distributions of maternal and paternal chromosomes to determine chromosome congression by measuring the ellipsoid's shortest axis. (B) Length of the ellipsoids shortest axis measurements of maternal and paternal chromosomes over time (n=12). (C) Correlation of maternal and paternal chromosome congression is plotted. Correlation coefficient (r) of chromosome congression over time for 12 embryos are shown. (r = 0: no correlation, r = 1: linear relationship, r = -1: negative correlation; for details see methods). (D) Schematic of angle measurements of maternal and paternal spindles. (E) Angles of the long axis of the paternal spindle versus the long axis of the maternal spindle during phase 1 and phase 2. (B, E) Phase 1, blue; Phase 2, red; Phase 3, green.

Supplementary Figure 3.Microtubule organization in pro-metaphase zygotes. (A) (i) Maximal Z and time projections of microtubule (MT) organisation in MMU x MMU embryos expressing the microtubule tip plus-end marker EGFP-EB3 in phase 2 and phase 3 (left upper and lower panel, respectively). (A) (ii) Kymographs computed along the yellow lines in (i) (width 1.43 µm, 11 pixels). The orange arrow indicates the spatial direction of the kymograph. The MT organisations in phase 2 embryo (a, b) and phase 3 embryo (c) show a typical criss-cross pattern indicating anti-parallel microtubule organisation as expected for spindles. To enhance the contrast the kymographs have been computed from a maximal Z projection of the EGFP-EB3 signal filtered with a Laplacian of Gaussian filter of radius 2. (B) EB3 tracks color coded according to the microtubule growth direction angle (left panel). The right panel shows EB3 tracks clustered according to their similarity. .

Supplementary Figure 4. Distribution of parental chromosomes in mouse zygotes. Differential labelling of maternal (magenta) and paternal (cyan) centromeres through distinction of minor and major satellite regions by fluorescent TALEs. Chromosome arms are labelled with H2B-mCherry (grey). Representative z-projected imagees of parental chromosome distribution on the metaphase plate of live imaged MMU x MSPS zygotes, 2-cell, 4-cell and 8-cell embryos are shown. Scale bar, 10 µm. (B) Schematic of 3D convex hull measurement used to determine degree of mixing between parental chromosomes. (C) Schematic of randomised parental centromere distributions at metaphase. (D) Degree of overlap between parental chromosomes at metaphase determined by 3D convex hull measurement for zygotes (n=31), 2-cell (n=20), 4-cell (n=20), 8-cell (n=12) embryos and embryos with *in silico* randomised distribution (n=40). (E) Distribution of paternal chromatin in MMU x MMU interphase nuclei. EdU-treated male mice were mated with untreated females and the resulting embryos stained for the incorporated EdU with Alexa Fluor 647 (green) by click chemistry and the nucleus counter stained with Sytox green (blue). Representative z-projected image for a 2-Cell embryo is shown. Scale bar, 10 µm. (F) Schematic of paternal chromatin distribution measurement. (G) Schematic of randomised paternal chromatin distribution at interphase. (H) Degree of paternal chromatin compartmentalisation at interphase measured for 2-cell (n=69), 4-cell (n=97), 8-cell (n=55) nuclei. (I) Degree of paternal chromatin compartmentalisation at interphase in randomised 2-cell, 4-cell and 8-cell nuclei (each n=40). (A-C,E-G, for details see methods). Difference in simulated values between D and H are caused by the different constraints of the arrangement on a metaphase plate or interphase nucleus (sphere) on the distribution of parental signal.

Supplementary Figure 5- Schematic summary of zygotic spindle assembly and experimental outline for achieving mixing of parental chromosomes during the first embryonic division. (A) Progressive transition from two bi-polar spindles to a single barrel shaped spindle. (B) Treatment of zygotes with Monastrol prior to NEBD brings maternal and paternal chromosomes into close proximity on a monopolar spindle. Subsequent washout into Nocodazole results in depolymerisation of microtubules. Washout of Nocodazole allows the spindle to reform in a random orientation leading to mixing of parental chromosomes. (C) Treatment of zygotes with Nocodazole prior to NEBD will result in maternal and paternal chromosomes condensing away from each other. Washout into Monastrol will result in maternal and paternal chromosomes aligning on a monopolar spindle. Washout of Monastrol will cause monopolar spindle to grow into bipolar spindle but separation of parental chromosomes will be maintained.

Supplementary Figure 6. Zygotic spindle formation in NocMo and MoNoc treated embryos. Live imaging of MMU x MSPS zygotes expressing fluorescent TALEs to label maternal (magenta) and paternal (cyan) chromosomes and EB3-mCherry (green). The first two panels show that a single bipolar spindle can be formed when a monopolar spindle collecting both parental genomes is first induced with Monastrol treatment prior to nuclear envelope breakdown, followed by transient microtubule depolymerisation with Nocodazole. The last two panels show that zygotes in which the drug treatment is reversed form two monopolar spindles upon Monastrol treatment that mature into one bi-polar spindle upon washout of the drug. Scale bars, 10μm.

Supplementary Figure 7. Intensity and distribution of 5mC and 5hmC in mixed and unmixed MMU x MMU embryos. (A) Immunofluorescence staining of zygotes, untreated, NocMo and MoNoc embryos at the 2-cell and 8-cell stage. Shown are z-projected images of confocal sections. Top panel shows 5mC and 5hmC staining (magenta, cyan) (salt and pepper distribution is expected based on results on parental chromosome distributions as determined in SF1 at the 2-cell stage). Middle panel shows DNA staining (white). Bottom panel shows chromosome surface (grey) and top 50% intensity pixels of 5mC (magenta) and 5hmC (cyan) printed as solid colours (see methods for details). Scale bar, 10 μm. (B) Volume occupied by top 50% 5mC positive voxels. (C) Volume occupied by top 50% 5hmC positive voxels. Zygote (n=16), untreated (n=26), NocMo (n=47) and MoNoc (n=39) cells at the 2-cell stage and untreated (n=30), NocMo (n=22) and MoNoc (n=35) cells at the 8-cell stage.

Supplementary Figure 8. Intensity and distribution of Ring1B and H3K9me3 in mixed and unmixed MMU x MMU embryos. (A) Immunofluorescence staining of zygotes, untreated, NocMo and MoNoc embryos at the zygote, 2- and 8-cell stage showing DNA (blue) and H3K9me (green). Shown are z-projected images of confocal sections. (B) Immunofluorescence staining of zygotes, untreated, NocMo and MoNoc embryos showing DNA (blue) and Ring1B (green). Shown are z-projected images of confocal sections. (C) Volume occupied by top 50% H3K9me3 positive voxels. Zygote (n=20), untreated (n=31), NocMo (n=41) and MoNoc (n=22) cells at the 2-cell and untreated (n=33), NocMo (n=44) and MoNoc (n=33) cells at the 8-cell stage. (D) Volume occupied by 50% Ring1B positive voxels. Zygote (n=17), untreated (n=37), NocMo (n=34) and MoNoc (n=19) cells at the 2-cell and untreated (n=11), NocMo (n=9) and MoNoc (n=10) cells at the 8-cell stage. Scale bar, 10 μm. Furthermore we re-implanted control, MoNoc and NocMo embryos into foster mothers and show that similar numbers of pups get born from each condition (Supplementary Table 1).

Supplementary Movies

Supplementary Movie 1
Live-cell time-lapse imaging of MMUxMSP mouse zygote expressing fluorescent TALEs for differential labelling of maternal (magenta) and paternal (cyan) centromeres through distinction of minor and major satellite regions. Chromosome arms are labelled with H2B-mCherry (grey). Time resolution is 7.5 min.

Supplementary Movie 2
Live-cell time-lapse imaging of MMU mouse zygote expressing EB3-mCherry (green) and tdEos-Cep192 (magenta). Time in min.

Supplementary Movie 3
Live-cell time-lapse imaging of mouse zygote 20 min after NEBD expressing EGFP-EB3 Time resolution is 800 ms

Supplementary Movie 4
Live-cell time-lapse imaging of mouse zygote 80 min after NEBD expressing EGFP-EB3. Time resolution is 800 ms.

Supplementary Movie 5-7
Live-cell time-lapse imaging of MMU mouse zygote after washout of Nocodazole (> 10 h treatment) expressing αTubulin-EGFP (green) and H2B-mCherry (magenta). Time resolution is 2 min.

Supplementary Tables

Supplementary Table 1. Frequency of pups born after re-implantion for untreated zygotes, zygotes treated transiently with Nocodazole followed by Monastrol (NocMo) and zygotes treated transiently with Monastrol followed by Nocodazole (all zygotes were collected from MMU x MMU crosses).